Christopher Kovalchick
Graduate Aerospace Laboratories,
California Institute of Technology,
Pasadena, CA 91125
e-mail: Kovalchick@gmail.com

Alain Molinari
Laboratoire d'Etude des Microstructures
et de Mécanique des Matériaux,
UMR 7213, Université de Lorraine,
Ile du Saulcy,
Metz Cedex 01 57045, France
e-mail: alain.molinari@univ-lorraine.fr

Guruswami Ravichandran[1]
Graduate Aerospace Laboratories,
California Institute of Technology,
Pasadena, CA 91125
e-mail: ravi@caltech.edu

Rate Dependent Adhesion Energy and Nonsteady Peeling of Inextensible Tapes

Elastomer based pressure sensitive adhesives used in various peeling applications are viscoelastic and expected to be rate sensitive. The effects of varying peel velocity on adhesion energy and its dependence on the peel angle and rate of peeling are investigated. Experiments are conducted on an adhesive tape using a displacement-controlled peel test configuration. By adjusting the peel arm length, the peel velocity can be continuously varied though the extremity of the film is displaced at a constant rate, which results in nonsteady peeling. Constant peel rate tests are performed over a wide range of peeling rates for a fixed peeling angle, which results in steady state peeling. Based upon the experimental data, a power law relation for the adhesive energy of a packaging tape and its dependence on the rate of peeling is presented. The applicability of the rate dependent law for adhesion energy based upon the steady state experiments to the nonsteady peeling process is critically examined. [DOI: 10.1115/1.4025273]

1 Introduction

Peeling is an important and ubiquitous process in biology and engineering [1–6]. For a nominally inextensible film, the peel strength is controlled by the peel angle and the adhesion energy of the film attached to the substrate [7]. Numerous investigations have been performed in understanding the mechanics of peeling, including the effects of extensibility, prestrain, large deformation, plasticity, and process zone [8–12]. The adhesives used in numerous engineering applications are characterized to be pressure sensitive and are based on elastomers. These elastomers are viscoelastic in nature [1,13,14] and, hence, exhibit rate dependent behavior. Such a rate dependence of adhesion has been also observed in other types of adhesive contact, as has been noted in transfer printing [3,15]. Though numerous investigations have been performed in determining the strength of adhesives based on steady state peeling tests (constant rate of peeling) (see, e.g., Ref. [16]), relatively little is known concerning the dependence of the adhesion energy on the rate of peeling. Such information is essential in understanding unsteady peeling processes encountered in many areas of engineering applications, including packaging, wafer bonding, transfer printing [3], gecko adhesion problem [4,5], and cell motility [6], among others.

The effects of varying peel velocity on the adhesion energy and its dependence on the peel angle and rate of peeling are investigated. A brief summary of theoretical results used in deducing the experimental data is presented in Sec. 2. The experiments are conducted using a displacement controlled peel testing configuration described in Sec. 3. By adjusting the peel arm length, the rate of peeling can be continuously altered, though the extremity of the film is displaced at a constant rate. This results in a continuously varying peel angle, which provides the additional insights presented in Sec. 4. In addition, constant peel rate tests are performed over a wide range of peeling rates of practical interest for a fixed peeling angle and the results are discussed. Based on the experimental data, a power law relation for the adhesive energy of a packaging tape and its dependence on the rate of peeling is presented. The validity of using steady state peeling data to model a nonsteady peeling process, such as in the case where the peeling angle and tip velocity continuously change, is critically examined.

2 Adhesion Energy and Peel Strength

In the analysis of the experiments presented here, the tape is assumed to be inextensible and the adhesion energy is given by Rivlin [7]

$$\gamma = \frac{F}{b}(1 - \cos\theta) \tag{1}$$

where γ is the adhesion energy per unit surface area, F is the total peel force, b is the width of the tape, and θ is the peel angle with the horizontal, i.e., the angle made by the tape extremity to the substrate. The adhesion energy γ for a linear elastic extensible tape adhered to a substrate is given by Kendall [17]

$$\gamma = \frac{F^2}{2Eb^2h} + \frac{F}{b}(1 - \cos\theta) \tag{2}$$

where E is the Young's modulus of the tape material and h is the thickness of the tape. The assumption of inextensibility of the tape will be examined later in light of the experimental results.

3 Experimental

3.1 Material and Geometry. The material used in the investigation is Scotch™ 3450S-RD Sure Start Shipping Packaging Tape (3 M, Minneapolis, MN), which has a width $b = 48$ mm (1.88 in.) and a thickness $h = 66\,\mu$m (0.0026 in.). This specific tape is used because of its relatively large width for which out-of-plane deformation and twisting during peeling is negligible and thus produces more consistent results.

3.2 Experimental Setup and Characterization. The tests are conducted using the experimental setup, shown schematically and pictorially, in Figs. 1(*a*) and 1(*b*), respectively. Using this setup, the extremity of the tape is vertically displaced at a prescribed velocity. A fixture made from delrin (a commercial plastic) is used to grip the tape, which is attached to the load cell (ALD-MINI-UTC-M, AL Design, Inc., Buffalo, NY). The load cell is screwed into the end of an aluminum peel arm, which is attached to a motorized translation stage (M-410.CG, Physik Instrumente, Irvine, CA). The stage has a total travel range of 100 mm, a maximum velocity of 1 mm/s, and a resolution of 100 nm. The stage is vertically mounted to an optical rail and used

[1]Corresponding author.

Manuscript received July 16, 2013; final manuscript received August 16, 2013; accepted manuscript posted August 22, 2013; published online October 16, 2013. Editor: Yonggang Huang.

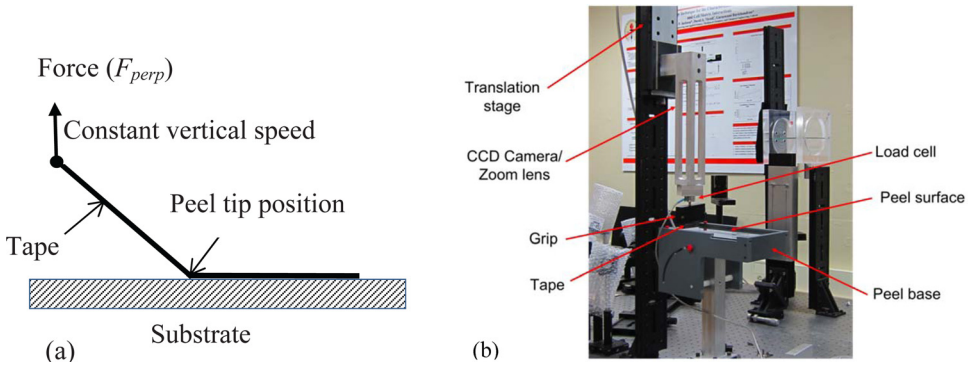

Fig. 1 Peel test configuration for studying the rate dependence of adhesion energy: (*a*) schematic and (*b*) photograph of the setup

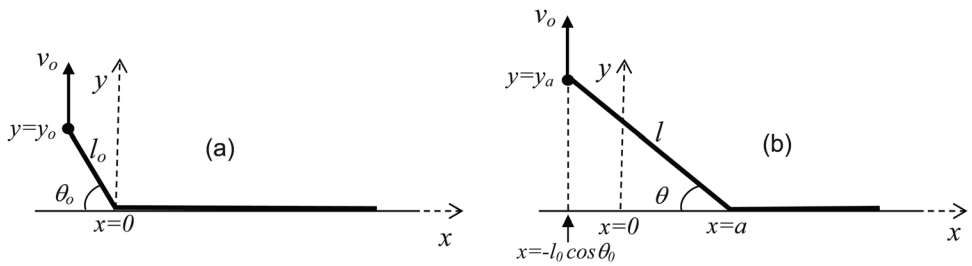

Fig. 2 Schematic of a displacement-controlled peel test at constant vertical velocity v_0 applied to the extremity of the tape whose horizontal location remains fixed at $x = -l_0 \cos\theta_0$: (*a*) initial configuration, and (*b*) current configuration

to apply a crosshead displacement, which peels the tape at a constant rate from a rigid glass plate with the dimensions of $203 \times 127 \times 3.175$ mm^3 (8 in. $\times$ 5 in. $\times$ 1/8 in.) for the length, width, and thickness, respectively. The initial peel angle can be altered by swiveling and locking the peel base made of delrin upon which the glass substrate is mounted. Prior to testing, the glass surface to which the tape is attached is cleaned with acetone, followed by wiping with isopropanol, and left to dry. The adhesive tape is then applied with care (to ensure repeatability) to the glass substrate with a roller and the adhesive is left to rest for 20 min prior to testing. Additional details of the peel test setup used in the study can be found elsewhere [18].

Three separate types of tests on Scotch^{TM} 3450 S-RD Sure Start Shipping Packaging Tape (3 M, Minneapolis, MN) are performed using the peel test setup. The width and thickness of the tape are 48 mm (1.88 in.) and 66 μm (2.6 mil), respectively. The first set examines the dependence of the peel force and adhesion energy on the peel velocity through a range of continuously varying angles. Using the setup in Fig. 1, tests are conducted for varying initial peel velocities (10–50 μm/s) with a short initial peel arm length of 12.7 mm (0.5 in.). As the translation stage is moved vertically, there is a rapid change of the peel angle. While a steady-state peel force is never reached, these experiments provide a means to study how the peel force and adhesion energy change with the angle as the angle is reduced from 90 deg towards 0 deg in a single test.

The second set of tests is performed using a longer peel arm so that the peel angle remains nearly constant. The goal of these tests is to measure the steady-state peel force (F) for a range of angles and contrast the results with those for the Scotch 810 Magic Tape [18]. The adhesion energy is also plotted as a function of the peel angle, in order to examine the question of whether or not the adhesion energy is a function of the peel angle. Finally, a set of measurements is conducted to examine the relation between the steady-state peel force and the prescribed peel velocity for tests with a constant peel angle of 90 deg. The data is used to develop a rate-dependent law that relates the peel force (adhesion energy) and the peel velocity.

3.3 Influence of Peel Arm Length on Peel Angle. Typically, peel tests are conducted while keeping the peel angle constant during a test in order to achieve a steady-state peel force at the given angle. This is done to compare the results to the predictions by the Rivlin and Kendall models [7,17] and also used to determine the peel strength of adhesive joints [2]. One way to achieve the constant peel angle is by having a long peel arm, since it can be seen, geometrically, that this enables the peel angle to be kept constant without moving the base upon which the rigid substrate is held. However, the peel angle can be rapidly changed by making the peel arm very short. Consider the case of a peel test shown in Fig. 2. The extremity of the tape is subjected to a constant velocity v_0 and is vertically displaced (pulled) in order to initiate and propagate the peel. The test begins in the undeformed (initial) configuration (see Fig. 2(*a*)), with the defined parameters including the initial peel arm length l_0, initial tip position (arbitrarily chosen as $x = 0$), initial peel angle θ_0, and the vertical position of the extremity $y = y_0$. The tape is peeled through some distance to the deformed (current) configuration (see Fig. 2(*b*)), where the instantaneous peel arm length, peel front tip position, peel angle, and the vertical position of the extremity are denoted by l, $x = a$, θ, and $y = y_a$, respectively. For an inextensible tape, the instantaneous peel arm length can be expressed as $l = l_0 + a$ since a is the displacement of the extremity of the tape. In addition, note that the origin is fixed in space reflecting the fact that the peel base is not moving with respect to the linear actuator, which displaces the extremity in the vertical direction.

From the geometry, the current peel angle θ (assuming inextensibility) is given by

$$\theta = \cos^{-1}\left(\frac{l_0 \cos\theta_0 + a}{l_0 + a}\right) \tag{3}$$

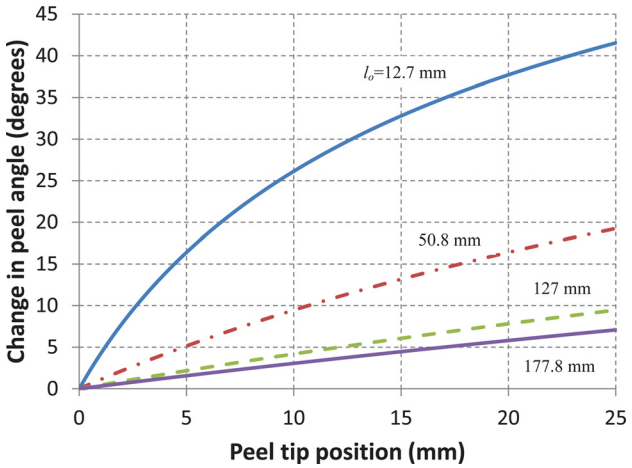

Fig. 3 Change in the peel angle $\theta_0 - \theta$ versus tip position a for the initial peel angle $\theta_0 = 90$ deg and varying initial peel arm lengths l_0 indicated in the plot

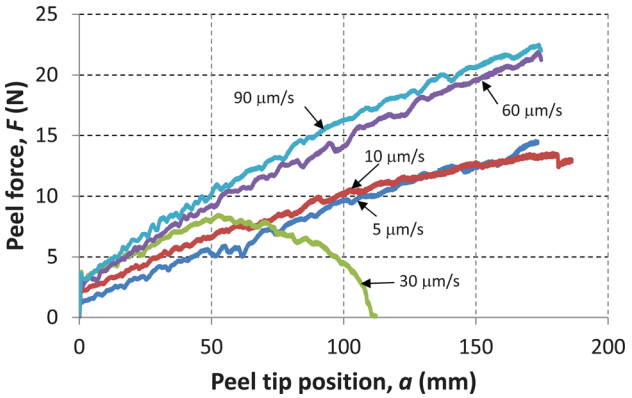

Fig. 4 Peel force F versus the peel tip position a for various prescribed extremity velocities (v_0) indicated in the plot. The test at $v_0 = 30$ μm/s is for a variable width tape, with the width decreasing at $x_c = 50$ mm.

Note that the peel angle is only related to the tip position (a) and the initial peel arm length (l_0) and peel angle (θ_0). The influence of the initial peel arm length on the change in the peel angle (using Eq. (3)) is seen in Fig. 3 over a range of tip positions for an initial peel angle $\theta_0 = 90$ deg and a varying initial peel arm length l_0. As l_0 is increased, the change in the peel angle ($\theta_0 - \theta$) for a given tip position ($x = a$) decreases. To keep the peel angle during a test at an intended constant value, l_0 is typically set to 76.2 mm (3 in.). In this case, the change in peel angle is less than 5 deg when the peel front advances by 10 mm. For a peel arm of $l_0 = 12.7$ mm (0.5 in.), the peel angle deviates from the initial peel angle ($\theta_0 = 90$ deg) by over 40 deg for a change in the peel tip position (debonded length) of 25 mm (see Fig. 3).

Since the peel arm length is changing, the peeling rate (tip velocity $\dot{a} = da/dt$)) also changes, even for a constant prescribed velocity at the extremity ($v_0 = dy_a/dt$) and are related to each other through the geometry

$$\dot{a} = \frac{da}{dt} = \frac{y_a}{l_0(1-\cos\theta_0)}\frac{dy_a}{dt} = \frac{\left(\sin\theta_0 + \dfrac{v_0 t}{l_0}\right)}{(1-\cos\theta_0)}v_0 \tag{4}$$

By integrating Eq. (4), the peel tip position can be obtained as a function of time

$$a = \frac{v_0 t}{(1-\cos\theta_0)}\left(\sin\theta_0 + \frac{v_0 t}{2l_0}\right) \tag{5}$$

Note that although the extremity of the tape may be displaced at a constant rate (v_0), the peel velocity ($\dot{a}$) is not constant, especially for an initially short peel band arm length (l_0). In addition, the peel angle is also continuously changing (see Eq. (3)), which also affects the peel velocity. The derivation of Eqs. (4) and (5) can be found in the Appendix.

4 Results and Discussion

4.1 Varying Peel Angle Tests Including Effect of Variable Width. Tests are conducted where the peel angle is forced to change very quickly in a single peel test by choosing the initial peel arm length (l_0) and peel angle (θ_0) to be 12.7 mm (0.5 in.) and 90 deg, respectively. This will allow the tip (peel front) velocity to change as a function of the angle while the applied extremity velocity (v_0) remains constant. It also allows for the examination of the peel force and adhesion energy for a range of angles through which the tape is being forced to move. Thus, there is less time for the adhesive to react and it is being forced to respond to the instantaneous tip velocity. This is in contrast to the constant-angle peel tests where equilibrium is reached and the values for these quantities are taken from the steady state. Though steady-state peeling is never achieved, the continuously varying angle tests provide insights concerning the rate-dependence of adhesion. For example, in the case when the peel angle changes from an initial value of $\theta_0 = 90$ deg to $\theta = 20$ deg, the tip velocity increases approximately fivefold over the prescribed constant velocity at the extremity $v_0 = 10$ μm/s (see Eq. (4) and the Appendix).

In one set of experiments, a new parameter is introduced; namely, a variable width for the adhesive tape. The width of the tape is usually kept constant (recall that for the packing tape $b = 48$ mm). Here, a linear decrease in width is introduced at a point where the tip position $x = a_c = 50$ mm from the beginning of the test ($x = 0$). The variable tape width is a linear function of the peel tip position (a), $b = b_0 - (2/5)(a - a_c)$ (for $0 < (a - a_c) < (5/2)b_0$) where b_0 is the initial constant width of the tape (in this case, 48 mm). The variable width provides additional insights on the dependence of the adhesion energy on the peel rate and stability of the debonding process.

Peel tests are conducted with the Scotch packaging tape for both constant and variable width sections. Several extremity velocities are applied: $v_0 = 5$, 10, 30, 60, and 90 μm/s. For the extremity velocity of $v_0 = 30$ μm/s, the variable width tape was used, while in all other cases, a tape with constant width was employed. A plot of the peel force (F) versus peel tip position (a) is shown in Fig. 4 for the various imposed extremity velocities.

For a given extremity (applied) velocity, the peel force increases in all cases with tip position, which is a result of the decreasing peel angle. Since there exists a point where the angle will not change appreciably anymore regardless of how long the tip propagates, the peel force approaches the steady-state condition. It is also clear that the peel force for a given tip position increases as the tip velocity increases. Looking specifically at the peel velocity $v_0 = 30$ μm/s, the change in width that commences at $x_c = 50$ mm also has an effect on the peel force. The peel force approaches zero at some tip position since the tape at this point is peeled completely off of the glass substrate. The adhesion energy γ is plotted as a function of the peel angle in Fig. 5. The adhesion energy γ is computed using the Rivlin relation (see Eq. (1)) from the data for the peel force ($F = F_{\text{perp}}/\sin\theta$) computed from the load cell data (F_{perp}) shown in Fig. 4 and the peel angle (θ) is computed using Eq. (3).

The adhesion energy appears to increase as a function of the peel angle for a prescribed extremity velocity. For a given peel

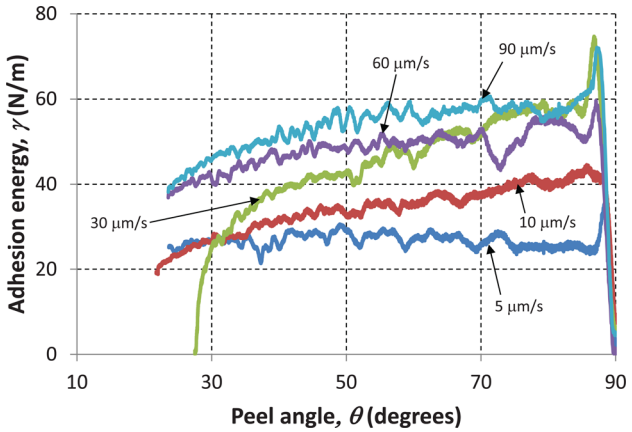

Fig. 5 Adhesion energy γ versus peel angle θ for varying extremity velocities (v_0) denoted on the plot. The tests are all conducted on constant width tapes except for $v_0 = 30\ \mu$m/s, where a variable width tape with the width decreasing at $x_c = 50$ mm is used.

angle, the adhesion energy increases as a function of the extremity velocity. Based upon these results, it can be hypothesized that the adhesion energy depends upon both the peel tip velocity and the peel angle (e.g., $\gamma\ (\dot{a}, \theta)$). However, it must be noted that the tip velocity and the peel angle are not independent of each other (see Eqs. (3) and (4)). Several previous studies assume the adhesion energy to be constant with respect to the peel angle (e.g., [16]). In order to examine this, separate measurements are conducted which examine γ as a function of $\dot{a}$ and θ independently. The change in width of the tape implemented in the $v_0 = 30\ \mu$m/s test is investigated in more detail elsewhere to investigate its implications for the stability of peeling [18,19]. This has also been theoretically discussed by Molinari and Ravichandran [20].

4.2 Constant Peel Angle Tests. As a result of the tests and observations in the previous section, the relationship between the adhesion energy γ with both the extremity velocity v_0 and the peel angle θ need to be investigated independent of each other. This is achieved by conducting peel tests at constant angles, keeping the velocity constant for a given test at a given angle. Peel tests are conducted for a range of angles of 30 deg to 90 deg at constant applied velocities to the extremity of $v_0 = 10\ \mu$m/s and $v_0 = 50\ \mu$m/s. The initial peel arm length is chosen to be in the range of $l_0 = 76.2$ mm (3 in.) to 114.3 mm (4.5 in.), which ensures a nominally constant peel angle during debonding. It should be noted that when the peel arm length is sufficiently large, the debonding speed (peel velocity $\dot{a}$) is related to the applied vertical velocity at the extremity of the tape (v_0) by the relationship

$$\dot{a} = v_0 \frac{\sin\theta_0}{(1 - \cos\theta_0)} \tag{6}$$

In all of the tests, the total tip propagation (debonding length) is 6 mm and the change in the peel angle is less than 2 deg. Hence, in all of these tests, the peel angle is assumed to be constant. The measured steady-state peel force F is plotted versus the peel angle θ and is shown in Fig. 6. The experimental data are plotted by the symbols, along with the Rivlin expression (see Eq. (1)), which is shown by the lines with values of the adhesion energy γ chosen to fit each curve.

Figure 6 illustrates a clear dependence of the steady-state peel force F on the prescribed velocity at the extremity v_0. For both the prescribed extremity velocities used here, the Rivlin relation fits the data quite well, assuming a constant value (with respect to θ) of the adhesion energy γ. By the choice of the long length of the

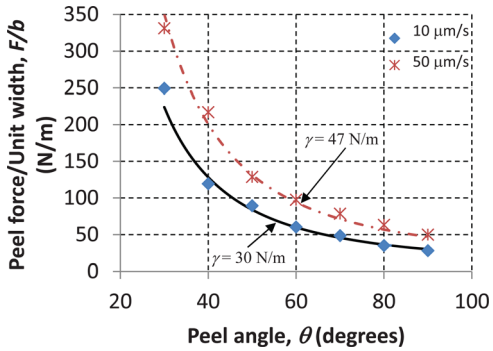

Fig. 6 Steady-state peel force/unit width (F/b) versus the peel angle (θ) for vertical velocities applied at the extremity of the tape of $v_0 = 10\ \mu$m/s and 50 μm/s for Scotch packaging tape. The symbols represent the experimental measurements and the lines are the best fit of the Rivlin relation in Eq. (1).

peel arm, the peel angle is kept relatively constant and, hence, the peel velocity also remains a constant in a given test.

In our attempts to make measurements at lower peel angles (<20 deg), it is very difficult to obtain steady-state peel-force values. This is so because of the effect of the extensibility at lower angles. To keep the peel angle constant at these lower angles, the peel arm length must be increased. As the peel angle approaches 0 deg, essentially a tensile test of the tape is being conducted, as opposed to a peel test.

The adhesion energy as a function of the rate and peel angle is also investigated. Figure 7 is a plot of the adhesion energy γ versus the peel angle θ for the same tests as in Fig. 6. The adhesion energy shown here is calculated using the Rivlin relation (see Eq. (1)) from the experimentally measured steady-state peel force F in Fig. 6, together with the prescribed peel angle θ.

In addition to the tests conducted for the Scotch packing tape at given velocities, the plot includes data from the Scotch magic tape tests at the vertical velocity prescribed at the extremity of $v_0 = 10\ \mu$m/s for comparison [18]. For all three sets of data, the adhesion energy is nearly constant with respect to the peel angle for a given peel rate. Comparing the values of γ for the Scotch magic tape and packaging tape at $v_0 = 10\ \mu$m/s, the values are almost the same, suggesting that the two tapes have similar adhesive properties. There is more scatter in the data for the adhesion energy of the Scotch magic tape as compared to the packaging tape. This can be attributed to the different widths of the two tapes used for testing: $b = 19$ mm for the magic tape and $b = 48$ mm for the packaging tape. Because the magic tape is narrower, the effects of any slight misalignment in the experiment are amplified

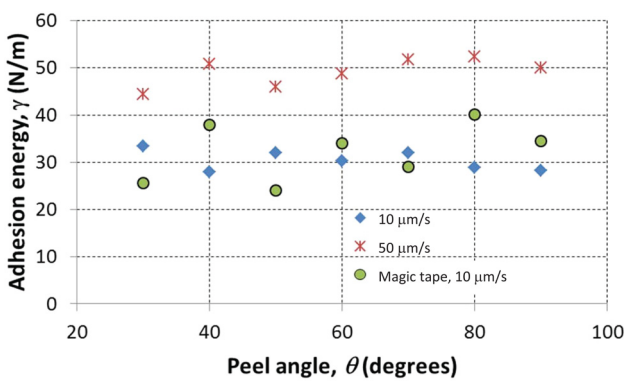

Fig. 7 Adhesion energy (γ) versus peel angle (θ) for vertical velocities applied at the extremity of the tape of $v_0 = 10\ \mu$m/s and 50 μm/s for Scotch packaging tape. For comparison, the data for the Scotch magic tape are also shown for the applied velocity at the extremity of the tape $v_0 = 10\ \mu$m/s [18].

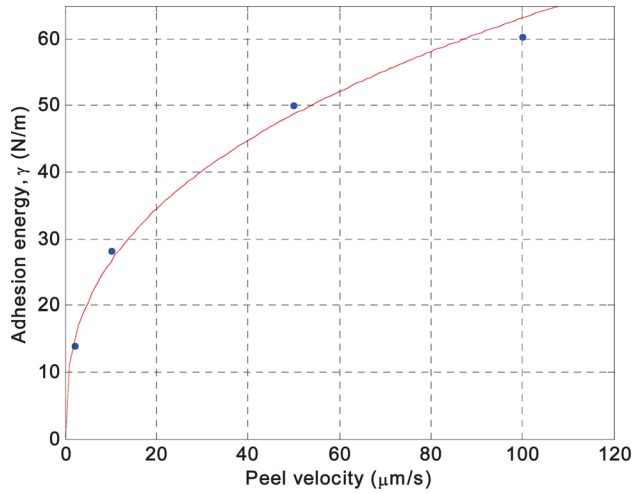

Fig. 8 Adhesion energy γ as a function of peel velocity $\dot{a}$. The symbols represent the experimental data and the solid curve is the best fit power-law relation (see Eq. (7)).

and can be a cause of more scatter in the results, as seen in Fig. 7. The backing materials of the two tapes also have similar elastic moduli, $E = 1.65$ GPa for the Scotch magic tape versus $E = 1.6$ GPa for the packaging tape [18]. The maximum strain in the peel tests in this study is 0.33% (computed using the data in Fig. 6) and, hence, the earlier assumption that the tape material is inextensible is validated.

Finally, a clear dependency of the adhesion energy on the peel velocity exists, since the adhesion energy for a given angle is greater for the peel tests at a higher applied velocity at the extremity of the tape. While γ is not a function of the peel angle, it is indeed a function of the peel velocity $\dot{a}$.

4.3 Rate-Dependent Relation for the Adhesion Energy. Based upon the results of the previous section, which show a clear dependency of the adhesion energy on the peel velocity, tests are conducted at several peel velocities using a constant-angle peel configuration with a constant peel angle $\theta = 90$ deg. The goal is to develop a rate-dependent law between the adhesion energy γ and the peel velocity $\dot{a}$ for a range of peel velocities. Figure 8 shows the adhesion energy plotted against the peel velocity for the prescribed vertical velocities of the extremity of $v_0 = 2$, 10, 50, and 100 μm/s for a peel angle of $\theta = 90$ deg. According to Eq. (6), the peel velocity is equal to the applied velocity at the extremity, $\dot{a} = v_0$. For this peel angle, the adhesion energy given by the Rivlin relation (see Eq. (1)) is equivalent to the peel force F per unit width, i.e., F/b.

The experimental data for the adhesion energy plotted as a function of the peel velocity in Fig. 8 can be described by a power-law expression (for the range of peel velocities considered here)

$$\gamma = \gamma_0 \left(\frac{\dot{a}}{\dot{a}_r} \right)^n \tag{7}$$

where $\dot{a}_r$ and γ_0 are reference values for the peel velocity and the corresponding value for adhesion energy, respectively. Here, n is the material rate dependence parameter, which, for the present study, is 0.376. For the material system, the reference values are $\gamma_0 = 11.2$ N/m and $\dot{a}_r = 1 \mu$m/s. Note that the Eq. (7) predicts zero adhesion energy as the peel velocity approaches zero. The empirical relation in Eq. (7) is applicable to only the range of peel velocities studied in this investigation. This rate-dependent relation for adhesion energy has been employed in earlier studies with the power-law dependence on the peel velocity [3,13–15], albeit with a different form and empirical constants.

4.4 Criterion for Steady State Peeling. The circumstances under which the steady-state condition might be applicable to transient peeling can be estimated by comparing the time $G/\dot{G}$ characterizing the variation of the energy release rate G with the travel time $\alpha/\dot{a}$ of the peel front through the process zone. Here, $\dot{a}$ is the peel front speed and α is the length of the cohesive zone. For crack propagation in viscoelastic materials, the steady-state solution applies during the propagation history of the crack, as long as the following relation holds [21]

$$\frac{\dot{G}(t)}{G(t)} \ll \frac{\dot{a}(t)}{\alpha(t)} \tag{8}$$

By transposing this relationship in the context of the debonding process and considering that $\dot{G}(t)/G(t) = \dot{\gamma}/\gamma$, the condition for steady state peeling takes the form

$$\frac{\dot{\gamma}(t)}{\gamma(t)} \ll \frac{\dot{a}(t)}{\alpha(t)} \tag{9}$$

Using Eqs. (7) and (9), it follows that

$$n \frac{\ddot{a}}{\dot{a}^2} \ll \frac{1}{\alpha} \tag{10}$$

Noting from Eq. (5) that $\dot{a}$ increases with time while $\ddot{a}$ is constant, one obtains

$$\frac{\ddot{a}(t)}{\dot{a}^2(t)} \leq \frac{\ddot{a}(0)}{\dot{a}^2(0)} = \frac{1 - \cos\theta_0}{l_0 \sin^2\theta_0} \tag{11}$$

Then, Eq. (10) is satisfied if

$$n \frac{1 - \cos\theta_0}{l_0 \sin^2\theta_0} \ll \frac{1}{\alpha} \tag{12}$$

Consider the adhesive tapes in the present investigation for which $n = 0.376$ (see Sec. 4.3) and $\theta_0 = 90$ deg, the condition for steady state peeling (see Eq. (12)) reduces to

$$0.376\alpha \ll l_0 \tag{13}$$

The size of the cohesive zone (α) for peel angles of 30 deg to 90 deg is typically in the range of 0.4–0.6 mm for Scotch magic tape, which has characteristics similar to the Scotch packaging tape used in the present study [18]. This suggests that nominally steady-state conditions prevail for the experiments discussed in Sec. 4.1 (see Figs. 4 and 5) since the initial peel arm length (l_0) is 12.7 mm, which is much greater in value in comparison to the length scale suggested by the foregoing analysis (left hand side of Eq. (13)), which is in the range 0.15–0.23 mm.

5 Conclusions

The effect of the peeling rate on the peel force during the peel test for a tape adhered to a rigid glass substrate is investigated. An experimental setup, which can cause rapid changes in the peel angle by employing a short initial peel arm, is utilized. Three sets of experiments are conducted in order to specifically investigate the relationship between the adhesion energy, the peel angle, and the peel velocity. The experiments where the peel angle is rapidly changed suggests a dependence of the adhesion energy γ on the peel velocity $\dot{a}$ and the peel angle θ. Further experiments using a constant rate of peeling showed that at a constant peel velocity, the adhesion energy remained constant for the entire range of the tested peel angles. Finally, experiments conducted at a constant

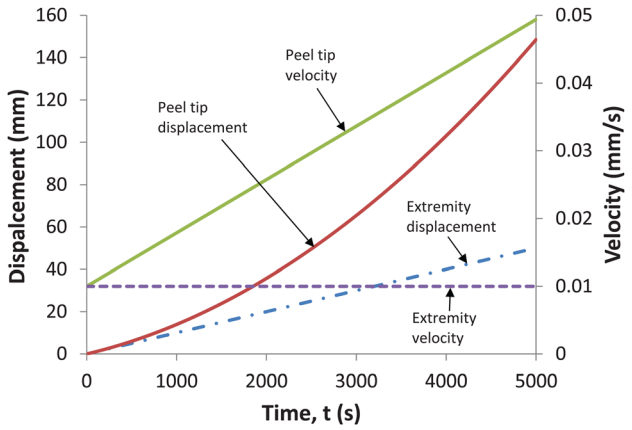

Fig. 9 Displacement and velocity (extremity (v_0), peel tip ($\dot{a}$)) versus time (t) in a displacement controlled peel test for an initial peel arm length of $l_0 = 12.7$ mm (0.5 in.) and an initial peel angle of $\theta_0 = 90$ deg. A constant vertical velocity ($v_0 = dy_a/dt$) is applied at the extremity of the tape (10 μm/s).

peel angle of 90 deg for varying velocities showed a clear power-law rate-dependency of the adhesion energy on the peel velocity. The rate dependent nature of the adhesion energy can be attributed to the viscoelastic characteristics of the elastomeric adhesive [1,13].

Acknowledgment

C.K. acknowledges the support through the National Defense Science and Engineering Science Graduate (NDSEG) Fellowship. A.M. wishes to express his appreciation for the hospitality provided during his visits to Caltech. G.R. gratefully acknowledges the support provided by the National Science Foundation (Grant No. CMMI-1201102).

Appendix: Relation Between Prescribed Velocity at the Extremity and Peel Velocity

Consider the displacement controlled peel test described and shown schematically in Fig. 2. An expression for the peel tip velocity ($\dot{a}$) during a peel test as a function of the prescribed velocity of the extremity of the tape at vertical position $y = y_a$, which was initially at $y = y_0$, is derived here.

Assuming an inextensible tape with the following quantities defined: θ_0 and θ are the initial and instantaneous peel angles, respectively; here, a is the displacement of the peel front tip due to debonding. Here, l_0 and l are the initial and instantaneous peel arm lengths, respectively, and are related through the following relation

$$l = l_0 + a \tag{A1}$$

From the geometry (see Fig. 2), the following relations are readily obtained

$$y_a = (l_0 + a)\sin\theta \tag{A2}$$

$$l^2 = (l_0\cos\theta_0 + a)^2 + y_a^2 \tag{A3}$$

Substituting Eq. (A1) into (A3)

$$(l_0 + a)^2 = (l_0\cos\theta_0 + a)^2 + y_a^2 \tag{A4}$$

Differentiating Eq. (A4) with respect to time (t)

$$2(l_0 + a)\frac{da}{dt} = 2(l_0\cos\theta_0 + a)\frac{da}{dt} + 2y_a\frac{dy_a}{dt} \tag{A5}$$

To simplify, an expression for the tip velocity can be obtained as

$$\frac{da}{dt} = \frac{y_a}{l_0(1-\cos\theta_0)}\frac{dy_a}{dt} \text{ or } \dot{a} = \frac{\left(\sin\theta_0 + \frac{v_0 t}{l_0}\right)}{(1-\cos\theta_0)}v_0 \tag{A6}$$

Integrating Eq. (A6), the peel tip position can be obtained as a function of time, in terms of the initial geometry of the tape and the prescribed velocity at the extremity

$$a = \frac{v_0 t}{(1-\cos\theta_0)}\left(\sin\theta_0 + \frac{v_0 t}{2l_0}\right) \tag{A7}$$

The initial condition is assumed to be $a = 0$ at $t = 0$. An example of the evolution of displacement and velocity (for the tape extremity and the peel tip) is shown as functions of time in Fig. 9.

References

[1] Benedek, I., 2004, *Pressure-Sensitive Adhesives and Applications*, Marcel Dekker, New York.
[2] ASTM D903-98, 2010, "Standard Test Method for Peel or Stripping Strength of Adhesive Bonds," ASTM International, West Conshohocken, PA.
[3] Meitl, M. A., Zhu, Z. T., Kumar, V., Lee, K. J., Feng, X., Huang, Y. Y., Adesida, I., Nuzzo, R. G., and Rogers, J. A., 2006, "Transfer Printing by Kinetic Control of Adhesion to an Elastomeric Stamp," Nature Mater., **5**, pp. 33–38.
[4] Tian, Y., Pesika, N., Zeng, H., Rosenberg, K., Zhao, B., McGuiggan, P., Autumn, K., and Israelachivili, J., 2006, "Adhesion and Friction in Gecko Toe Attachment and Detachment," Proc. Natl. Acad. Sci. U.S.A., **103**, pp. 19320–19325.
[5] Yao, H. and Gao, H., 2006, "Mechanics of Robust and Releasable Adhesion in Biology: Bottom-Up Designed Hierarchical Structures of Gecko," J. Mech. Phys. Solids, **54**, pp. 1120–1146.
[6] Garrivier, D., Decave, E., Brechet, Y., Bruckert, F., and Fourcade, B., 2002, "Peeling Model for Cell Detachment," Eur. Phys. J. E, **8**(1), pp. 79–97.
[7] Rivlin, R. S., 1944, "The Effective Work of Adhesion," J. Paint Technol., **9**, pp. 215–218.
[8] Thouless, M. D. and Yang, Q. D., 2008, "A Parametric Study of the Peel Test," Int. J. Adhes. Adhes., **28**, pp. 176–184.
[9] Williams, J. A. and Kauzlarich, J. J., 2005, "The Influence of Peel Angle on the Mechanics of Peeling Flexible Adherends With Arbitrary Load-Extension Characteristics," Tribol. Int., **38**, pp. 951–958.
[10] Molinari, A. and Ravichandran, G., 2008, "Peeling of Elastic Tapes: Effects of Large Deformations, Pre-Straining, and Peel-Zone Model," J. Adhes., **84**, pp. 961–995.
[11] Kim, K. S. and Aravas, N., 1988, "Elastoplastic Analysis of the Peel Test," Int. J. Solids Struct., **24**, pp. 417–435.
[12] Wei, Y. and Hutchinson, J. W., 1998, "Interface Strength, Work of Adhesion and Plasticity in the Peel Test," Int. J. Fract., **93**, pp. 315–333.
[13] Gent, A. N. and Petrich, R. P., 1969, "Adhesion of Viscoelastic Materials to Rigid Substrates," Proc. R. Soc. London, Ser. A, **310**, pp. 433–448.
[14] Barthel, E. and Roux, S., 2000, "Velocity Dependent Adherence: An Analytical Approach for the JKR and DMT Models," Langmuir, **16**, pp. 8134–8138.
[15] Chen, H., Feng, X., Huang, Y., Huang, Y., and Rogers, J. A., 2013, "Experiments and Viscoelastic Analysis of Peel Test With Patterned Strips for Applications to Transfer Printing," J. Mech. Phys. Solids, **61**, pp. 1737–1752.
[16] Pesika, N. S., Tian, Y., Zhao, B., Rosenberg, K., Zeng, H., McGuiggan, P., Autumn, K., and Israelachivili, J. N., 2007, "Peel-Zone Model of Tape Peeling Based on the Gecko Adhesive System," J. Adhes., **83**, pp. 383–401.
[17] Kendall, K., 1975, "Thin-Film Peeling—The Elastic Term," J. Phys. D: Appl. Phys., **8**, pp. 1449–1452.
[18] Kovalchick, C., 2011, "Mechanics of Peeling: Cohesive Zone Law and Stability," Ph.D. thesis, California Institute of Technology, Pasadena, CA.
[19] Kovalchick, C., Molinari, A., and Ravichandran, G., 2013, "An Experimental Investigation of the Stability of Peeling for Adhesive Tapes," Mech. Mater., **66**, pp. 69–78.
[20] Molinari, A. and Ravichandran, G., 2013, "Stability of Peeling for Systems With Rate Independent Decohesion Energy," Int. J. Solids Struct., **50**, pp. 1974–1980.
[21] Knauss, W. G., 2003, "Viscoelasticity and the Time-Dependent Fracture in Polymers," *Comprehensive Structural Integrity, Vol. 2: Fundamental Theories and Mechanisms of Failure*, B. L. Karihaloo and W. G. Knauss, eds., Elsevier, Oxford, UK, pp. 383–428.